

This is a non-peer reviewed EarthArXiv preprint of a manuscript submitted to Environmental Science and Technology

1 Shining light on priming in euphotic sediments: Nutrient enrichment stimulates export of stored  
2 organic matter

3 Philip M. Riekenberg<sup>1,2\*</sup>, Joanne M. Oakes<sup>2</sup>, Bradley D. Eyre<sup>2</sup>

4

5 <sup>1</sup>NIOZ, Royal Netherlands Institute for Sea Research and Utrecht University, Department of  
6 Marine Microbiology and Biogeochemistry, PO Box 59, Den Hoorn, 1790AB, Netherlands

7 <sup>2</sup>Centre for Coastal Biogeochemistry, Southern Cross University, PO Box 157, Lismore, NSW,  
8 2480, Australia

9

10 \* Corresponding author: phrieken@gmail.com +31644994652

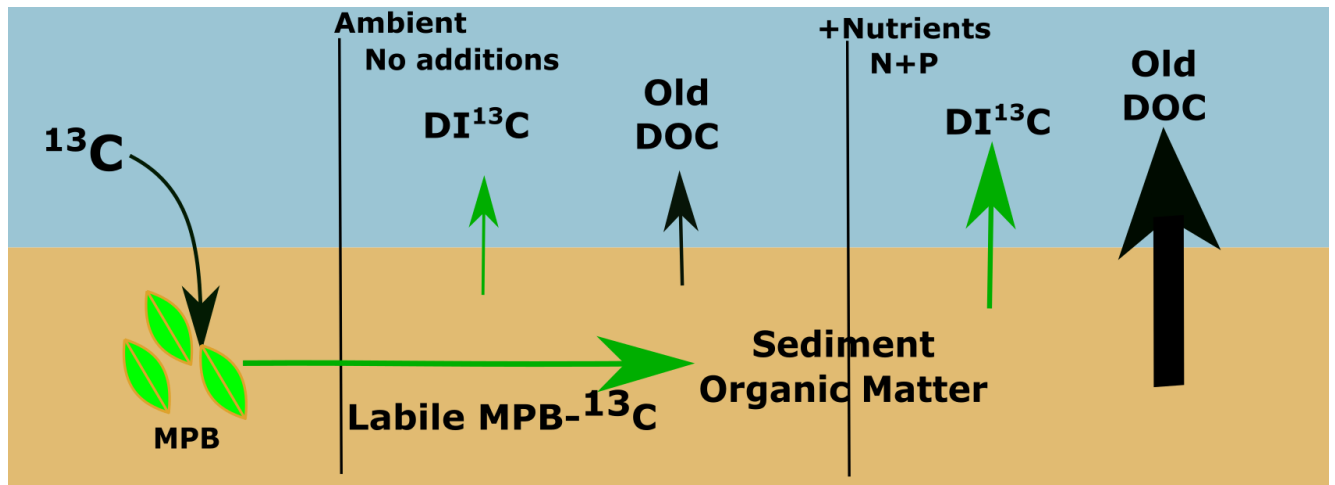
11

12 Keywords: nutrient enrichment, microphytobenthos, carbon, priming

13

14 Teaser: Priming effects drive increased export of organic carbon from refractory sediment  
15 organic matter in euphotic intertidal zones.

16 **Author created TOC graphic**



17  
18

19 **Estuarine sediments are important sites for the interception, processing and retention of**  
20 **organic matter, prior to its export to the coastal oceans. Stimulated microbial co-**  
21 **metabolism (priming) potentially increases export of refractory organic matter through**  
22 **increased production of hydrolytic enzymes. By using the microphytobenthos community to**  
23 **directly introduce a pulse of labile carbon into sediment, we traced a priming effect and**  
24 **assessed the decomposition and export of pre-existing organic matter. We show enhanced**  
25 **efflux of pre-existing carbon from intertidal sediments enriched with water column**  
26 **nutrients. Nutrient enrichment increased production of labile microphytobenthos-carbon**  
27 **which stimulated degradation of previously unavailable organic matter and led to increased**  
28 **liberation of “old” ( $6855 \pm 120$  years BP) refractory carbon as dissolved organic carbon.**  
29 **These enhanced DOC effluxes occurred at a scale that decreases estimates for global**  
30 **organic carbon burial in coastal systems and should be considered as an impact of**  
31 **eutrophication on estuarine carbon budgets.**

32

33

## 34 **Introduction**

35 Estuaries, and particularly shallow photic estuarine sediments (<40 m)<sup>1</sup>, are hotspots for  
36 organic matter (OM) processing, altering terrestrial OM received from rivers prior to its export to  
37 the coastal ocean<sup>2-4</sup>. The extent of terrestrial OM processing that occurs along the estuarine  
38 continuum largely determines whether estuaries function as carbon (C) sources or sinks<sup>4</sup>. The  
39 priming effect (PE) describes the additional release of C from a refractory source of OM (pre-  
40 existing sediment OM in this study, or added refractory material in others) stimulated by addition  
41 of a labile form of C. In terrestrial environments, increased C release from soils is usually  
42 measured as evolution of additional CO<sub>2</sub> into a headspace from amended treatments (with labile  
43 C added) when compared to non-amended controls<sup>5</sup>. Although PE has been well-described and  
44 explored within soils<sup>6</sup>, PE has only recently gained recognition in aquatic systems. Within  
45 aquatic sciences, PE has primarily been investigated as a potential pathway for additional OM  
46 processing within settings where heterotrophy dominates (e.g., riverine dissolved OM, hyporheic  
47 zone, deep sediment; Fig. 1)<sup>7-10</sup> and has not been consistently demonstrated to occur<sup>11</sup>.  
48 Occurrence of PE is highly dependent on substrate composition, sediment structure, and/or  
49 microbial community composition<sup>11</sup>. Studies examining priming within coastal benthos are  
50 limited<sup>8,12,13</sup>, but have found positive PEs within their limited scope (i.e., vial incubations of  
51 sediment slurries).

52 PE studies in aquatic environments have thus far relied on the evolution of <sup>13</sup>CO<sub>2</sub> from  
53 dissolved inorganic carbon (DI<sup>13</sup>C) derived from either labile or refractory C sources (study  
54 dependent) to quantify the relative contributions from microbial processing of the <sup>13</sup>C addition. A  
55 number of approaches have been used in various environments in an attempt to identify PEs, i.e.,  
56 to demonstrate that microbial degradation of refractory terrestrial organic C has been stimulated

57 following the addition of labile C<sup>10,14-16</sup>. These approaches use additions of both refractory OM  
58 and labile C to stimulate mineralization of added OM<sup>13,17</sup> or pre-existing sediment OM (Fig.  
59 2A)<sup>8,9,12,18</sup>. Addition of unlabeled C (refractory or labile) into the sediment confounds  
60 partitioning of export pathways by introducing new OM. Any exported C derived from this  
61 newly added OM is indistinguishable from that derived from pre-existing sediment OM. In this  
62 study, we used the in situ MPB community to inject a pulse of labile MPB<sup>13</sup>C into coastal  
63 sediments (Fig. 2B). This approach was intended to preserve both the production (loading rate)  
64 and composition (proportion of relative sugars) of priming additions produced daily by diatoms  
65 within highly productive shallow coastal environments<sup>12,19</sup>. This method preserves the microbial  
66 community, as boundary layers and sediment structure are maintained during label addition with  
67 minimal disturbance. This differs from all other PE studies, which have directly added single  
68 labile and/or refractory compounds to homogenized sediment (Fig. 2A)<sup>8,9,12,13,20</sup>.

69         Some PE studies account for both dissolved inorganic C (DIC) and dissolved organic  
70 carbon (DOC) pools when identifying additional stimulated breakdown and release of C<sup>8,14-16</sup>,  
71 but it remains common to solely measure the evolution of DI<sup>13</sup>C and DIC<sup>9,10,13,18</sup>. This approach  
72 works well for systems where heterotrophic evolution of DIC is the only or major pathway for C  
73 loss. However, relying on DIC effluxes alone to identify PE becomes problematic in systems  
74 where primary production during light exposure utilizes DIC at rates exceeding the evolution of  
75 respired DIC (Fig. 1B). This scenario occurs in shallow coastal benthic sediments, where there is  
76 considerable DIC demand by MPB during light periods, and can result in the re-capture and  
77 recycling of previously respired carbon. Strong uptake of DIC in euphotic settings could  
78 potentially be wrongly interpreted as a negative priming effect as labeled DIC is recycled and  
79 reincorporated into biomass instead of being evolved as <sup>13</sup>CO<sub>2</sub>. This is especially the case in

80 systems that are DIC-limited or have elevated rates of primary productivity due to  
81 eutrophication. We argue that recycling of DIC in euphotic situations can be partially offset by  
82 refining the definition of priming to encompass all C remineralized from refractory OM (i.e.,  
83 including DOC effluxes from sediment OM). In productive systems, heterotrophic bacteria are  
84 provided with rich algal-derived organic matter that can fuel breakdown of otherwise refractory  
85 pre-existing sediment OM as DOC. Measuring PEs using the evolution of DOC in addition to  
86 DIC from both labile and refractory OM sources will account for all substrates produced by the  
87 microbial community during remineralization.

88         From this study, we infer that: 1) amendment with nutrients (N as  $\text{NH}_4^+$  and phosphorous  
89 as  $\text{H}_3\text{PO}_4$ ) stimulated release of labile C by MPB, leading to a PE that released additional stored  
90 refractory carbon from coastal sediments, and 2) simultaneous monitoring of both DIC and DOC  
91 fluxes was required to detect this PE. Through consideration of both DIC and DOC fluxes, we  
92 determined that there was significantly increased export of both MPB<sup>13</sup>C and pre-existing C  
93 despite the high productivity evidenced by negative DIC fluxes (DIC uptake). We further  
94 confirmed that additional exported DOC was derived from previously stored refractory sediment  
95 OM. Interactions between MPB and heterotrophic bacteria, stimulated through an equimolar  
96 nutrient addition of N and P equivalent to 2.5× the trigger concentration for increased trophic  
97 status under ANZECC guidelines<sup>21</sup>, increased the export of old carbon to the continental shelf  
98 that would otherwise be considered “locked away” in sediment OM and unavailable for  
99 processing and export. This carbon was primarily exported as DOC, representing a poorly  
100 quantified pathway for increased mobilization of blue carbon in euphotic settings that could be a  
101 significant component of OC budgets for intertidal systems<sup>22</sup>.

102

## 103 **Methods**

104 In January 2015 a subtropical intertidal shoal was sampled ~2 km upstream of the mouth of the  
105 Richmond River estuary in New South Wales, Australia (28°52'30"S, 153°33'26"E). A number  
106 of previous labeling studies have been undertaken at this site<sup>33,36</sup>. Site sediment (0-10 cm) was  
107 mostly fine sand (66%-73%), with a total organic C content of  $17.5 \pm 0.02 \text{ mol C m}^{-2}$ , an average  
108 molar C:N ratio of  $14.7 \pm 1.5$ , and a MPB assemblage dominated by pennate diatoms. There was  
109 no evidence of cyanobacteria and few heterotrophs ( $>500 \mu\text{M}$ ) observed under light microscopy  
110 ( $1000 \times$ ). Foraminifera were the dominant heterotrophs ( $>500 \mu\text{M}$ ) within site sediment.

### 111 Labeling of MPB Exudates

112 We applied  $^{13}\text{C}$  to MPB *in situ* to track the production of algal carbon that occurred during a  
113 single tidal minimum within the intertidal setting in order to track production and processing of  
114 MPB derived C. Application of stable isotope (SI) tracer material (99%  $\text{NaH}^{13}\text{CO}_3$ ) during a tidal  
115 low allowed for incorporation across ~ 4 hours of  $1549 \pm 140 \mu\text{mol } ^{13}\text{C m}^{-2}$  into sediment OC  
116 followed by significant flushing of non-incorporated  $^{13}\text{C}$  from the sediment during tidal  
117 inundation of the site as confirmed by loss of 99.0% of the material in the label application based  
118 on measured incorporation in the sediment within the initial cores<sup>32</sup>. Of the  $^{13}\text{C}$  incorporated into  
119 sediment OC, ~46% or  $716 \mu\text{mol } ^{13}\text{C}$  is expected to be in the form of carbohydrates as  
120 calculated from uptake rates for  $^{13}\text{C}$  presented in [Oakes, et al.](#)<sup>19</sup> for mannose, fucose, rhamnose,  
121 galactose, glucose, xylose, and OC. Bare sediment within two experimental plots ( $1 \text{ m}^2$ ) was  
122 labeled with 99%  $\text{NaH}^{13}\text{CO}_3$  when sediments were first exposed at low tide, following the  
123 method outlined in [Oakes and Eyre](#)<sup>33</sup>. Label applications were prepared using NaCl-amended  
124 Milli-Q to match site salinity (34.6) and 20 mL aliquots ( $1.7 \text{ mmol } ^{13}\text{C}$ ) were applied to each

125 individual 400 cm<sup>2</sup> subplot, resulting in a label application of 42.5 mmol <sup>13</sup>C m<sup>-2</sup>. The use of  
126 motorized sprayers and individual aliquots of label ensured even <sup>13</sup>C application across the  
127 sediment surface. Assimilation of label by the sediment community occurred over ~4 hours  
128 during sediment exposure under an average light level of 1376 μE m<sup>-2</sup> s<sup>-1</sup>. Removal of  
129 unincorporated DI<sup>13</sup>C by tidal flushing was confirmed, with only ~1% of the initially added <sup>13</sup>C  
130 application found in the inorganic sediment C fraction within the initial cores prior to incubation.

### 131 Core Incubations

132 Sediment cores (20 cm depth, 9 cm diameter) were taken from the labeled plots on the second  
133 low tide after labeling, transported to the laboratory, randomly allocated between treatment tanks,  
134 and incubated under two nutrient enrichment scenarios (ambient and elevated) using 2 pulsed  
135 nutrient additions. Duplicate cores (n=2) were incubated for each time period (0.5 d, 1.5 d, 2.5 d,  
136 3.5 d and 10.5 d) for each treatment (ambient and elevated, total core n=20). Laboratory core  
137 incubations allowed explicit control of nutrient additions, reducing the variability in water quality  
138 that occurs naturally across the tidal cycle. Pulsed applications of nutrients were used to mimic a  
139 range of nutrient concentrations without exceeding sediment capacity for uptake <sup>32</sup>. NH<sub>4</sub><sup>+</sup> pulses  
140 were completely taken up within 24 h of application. Treatment tanks were set up at ambient  
141 concentration (site water), and with N (NH<sub>4</sub><sup>+</sup>) and P (H<sub>3</sub>PO<sub>4</sub>) amendment for the elevated  
142 treatment at 10 × water column concentrations observed previously for this site (4 μmol L<sup>-1</sup> TN  
143 and 5 μmol L<sup>-1</sup> TP). These loadings are ~2× equimolar concentrations observed in the Richmond  
144 River for both TN and TP in 2006 (25.8 μmol L<sup>-1</sup> and 24.5 μmol L<sup>-1</sup>, respectively) (<sup>33</sup>) and  
145 ~2.5× concentrations observed directly after flooding events in the Richmond River <sup>37</sup> and are  
146 comparable to increased nutrient loading observed in other estuaries subject to eutrophication <sup>38</sup>.  
147 The initial pulse of nutrients was added to incubation tanks and bags holding replacement water



148 for sampling shortly prior to cores being randomly allocated to the two incubation tanks. An  
149 additional pulse of  $\text{NH}_4^+$  was applied to the elevated treatment tank at the end of 1.5 d in an effort  
150 to mimic the nutrient availability that occurs with regular inundation of tidal sediments. An  
151 addition of sodium metasilicate ( $\text{Na}_2\text{SiO}_3$ ,  $17 \mu\text{mol Si L}^{-1}$ ) was added to both treatment tanks at  
152 the end of the 2.5 d to ensure that isolation of the benthic diatom-dominated sediment from  
153 regular water turnover did not result in secondary limitation of Si.

#### 154 Benthic flux incubations

155 Cores were fitted with magnetic stir bars positioned 10 cm above the sediment surface and filled  
156 with ~2 L of site water. Water in the treatment tanks and cores was continuously recirculated,  
157 held at  $25 \pm 1^\circ\text{C}$  by a chiller on each tank, and aerated via continuous direct injection of ambient  
158 air into the water via an air stone. Cores were stirred via a rotating magnet at the center of each  
159 treatment tank, which interacted with the magnetic stir bars fitted within each core. Stirring  
160 occurred at a rate below the threshold for sediment resuspension<sup>39,40</sup>. Three high pressure sodium  
161 lamps (correlated color temperature ~2100)<sup>41</sup> suspended above the treatment tanks provided  $824$   
162  $\pm 40 \mu\text{E m}^{-2} \text{ s}^{-1}$  to the sediment/water interface within the cores on a 12 h light/12 dark cycle.  
163 This light level is similar to the measured light level for the in situ site sediment surface during  
164 inundation ( $941.4 \pm 139 \mu\text{E m}^{-2} \text{ s}^{-1}$ ).

165 Cores were allowed to acclimate for 6 h before the incubation time began and remained open to  
166 the tank water until 30 min before initial sampling when clear Plexiglas lids were fitted to each  
167 core liner to seal in overlying water without headspace for the duration of the incubation. Rapid  
168 processing of the added MPB-C likely occurred during the 6 h acclimation period, but flux  
169 measurements were not possible during re-establishment of sediment redox layers immediately

170 after coring. The acclimation period allowed for a robust baseline to develop prior to sampling  
171 for diel water column flux incubations. During sampling, 50 mL of water was syringe-filtered  
172 (precombusted GF/F) into precombusted 40 mL glass vials with Teflon coated septa, killed with  
173  $\text{HgCl}_2$  (20  $\mu\text{L}$  saturated solution), and refrigerated prior to analysis for concentration and  $\delta^{13}\text{C}$  of  
174 DIC and DOC. Initial samples were taken 30 min after closure of the lids, dark samples were  
175 taken after ~12 hours incubation with no light, and light samples were taken 3 hours after  
176 illumination after the end of the dark sampling. Oxygen measurements were taken for the  
177 overlying water with oxygen saturation never occurring below 86.1% during the dark incubations  
178 (oxygen fluxes presented in [Riekenberg, et al.<sup>32</sup>](#)). DIC and DOC concentrations and  $\delta^{13}\text{C}$  values  
179 (‰) were measured via continuous-flow wet oxidation isotope-ratio mass spectrometry using an  
180 Aurora 1030W total organic C analyzer coupled to a Thermo Delta V isotope ratio mass  
181 spectrometer (IRMS)<sup>42</sup>. Sodium bicarbonate (DIC) and glucose (DOC) of known isotopic  
182 composition dissolved in He-purged Milli-Q were used to correct for drift and verify both  
183 concentration and  $\delta^{13}\text{C}$  of samples. Reproducibility was  $\pm 0.2 \text{ mg L}^{-1}$  and  $\pm 0.1 \text{ ‰}$  for DIC and  $\pm$   
184  $0.2 \text{ mg L}^{-1}$  and  $\pm 0.4 \text{ ‰}$  for DOC.

185 Total  $^{13}\text{C}$  in water column DIC and DOC was calculated for initial, the end of the dark period,  
186 and the end of the light period as the product of excess  $^{13}\text{C}$  (excess  $^{13}\text{C}$  in labeled sample versus  
187 relevant natural abundance control), core volume, and concentration. Total excess flux of  $^{13}\text{C}$  as  
188 DIC or DOC was then calculated as:

189 
$$\text{Excess } ^{13}\text{C} \text{ flux} = (\text{Excess } ^{13}\text{C}_{\text{start}} - \text{Excess } ^{13}\text{C}_{\text{end}}) / \text{SA} / t$$

190 where excess  $^{13}\text{C}_{\text{start}}$  and excess  $^{13}\text{C}_{\text{end}}$  represent excess  $^{13}\text{C}$  of DIC or DOC at the initial and dark  
191 samplings to calculate dark flux and the dark sampling to the end of the light incubation periods

192 to calculate the light flux, SA is sediment surface area, and  $t$  is incubation period length (h). Net  
193 fluxes of excess  $^{13}\text{C}$  (excess  $^{13}\text{C} \text{ m}^{-2} \text{ h}^{-1}$ ) for DIC and DOC were calculated as:

194 
$$\text{Net flux} = ((\text{dark flux} * \text{dark hours}) + (\text{light flux} * \text{light hours})) / 24 \text{ hours}$$

195 Total carbon fluxes for DIC and DOC as well as  $\text{DI}^{13}\text{C}$  and  $\text{DO}^{13}\text{C}$  exported to the water column  
196 from initial labeling to each sampling period was interpolated using measured net flux values for  
197 each treatment during each sampling period (0.5 d, 1.5 d, 2.5 d, 3.5 d, and 10.5 d). Carbonate  
198 dissolution made a negligible contribution to total  $\text{CO}_2$  during incubations and therefore no  
199 corrections were applied to DIC fluxes<sup>32</sup>.

200 Global flux estimates for DOC ( $\text{Tg C yr}^{-1}$ ) were calculated as in [Maher and Eyre<sup>23</sup>](#):

201 
$$\text{DOC}_{\text{Glob}} = 6.7 * (\text{DOC}_{\text{Net}} * \text{Inter}_{\text{Area}} * 365 * 12.011) / 10^{15}$$

202 where 6.7 represents the increased DOC flux observed from PEs in this study,  $\text{DOC}_{\text{Net}}$  are  
203 minimum and maximum average diel DOC fluxes observed in [Maher and Eyre<sup>23</sup>](#) (2.7 and 3.7  
204  $\text{mmol C m}^{-2} \text{ d}^{-1}$ ),  $\text{Inter}_{\text{Area}}$  is the global intertidal area  $0.62 (10^{12} \text{ m}^2)$ <sup>43</sup>, and 12.011 is the atomic  
205 mass of carbon required to convert from molar weight to grams of C.

## 206 Characterization of DOC Efflux

207 The UV-visible absorption spectra was measured from 300-700 nm on a Horiba Aqualog using a  
208 1 cm cell. Absorbance (A) is converted to absorption coefficients (a) using  $a_{(\lambda)} = 2.303 A(\lambda) / l$ ,  
209 where  $A(\lambda)$  is absorbance at wavelength  $\lambda$  and  $l$  is the path length of the cell in meters. Spectral  
210 slope was determined by fitting  $a_{(300-700)}$  to a single exponential decay function using non-linear  
211 regression<sup>24</sup>. The spectral slopes from both 275-295 nm ( $S_{275-290}$ ) and 350-400 nm ( $S_{350-400}$ ) were  
212 calculated through linear regression of the log transformed spectra. Slopes are reported as

213 positive numbers following mathematical convention. The slope ratio ( $S_R$ ) was calculated the  
214 ratio of  $S_{275-295}$  and  $S_{350-400}$ .  $S_R$  is inversely related to the molecular size of the chromophoric  
215 dissolved organic matter (CDOM) within the sample and is expected to increase with decreasing  
216 molecular size.

217 SUVA 254 ( $L\ mg^{-1}\ m^{-1}$ ) is an indicator of relative aromaticity of the molecules comprising the  
218 pool of CDOM <sup>25</sup> and is calculated as:

219 
$$SUVA\ 254 = a_{254} / DOC$$

220 where  $a_{254}$  is the absorption coefficient at 254 nm ( $m^{-1}$ ) and DOC is concentration of DOC ( $mg\ L^{-1}$ )  
221 within the sample. Elevated SUVA 254 indicates the increased presence of aromatic moieties  
222 contained within CDOM.

### 223 Radiocarbon dating of Dissolved Organic Carbon

224 Samples from the dark flux incubations from ambient (n=2) and elevated treatments (n=2) at 10.5  
225 d analyzed for  $^{14}C$  of DOC. The ambient samples failed to successfully graphitize during analysis  
226 and were lost. Samples were selected from the dark flux to target the high concentration  
227 measurements for DOC that occurred during respiration and to avoid the potentially confounding  
228 signal from newly produced EPS from diatoms that is expected during light periods. The  $^{14}C$ -  
229 DOC samples were analyzed by accelerator mass spectrometry at the Australian Nuclear Science  
230 and Technology Organisation<sup>44</sup>. DOC samples were acidified to  $pH < 2$  and dried under vacuum  
231 in a rotary evaporator. The residue was heated in a glass tube containing  $CuO$ ,  $Ag$ , and  $Cu$  wire  
232 to  $600^\circ C$  for 2 h to remove any sulfur compounds. The sample was then graphitized by reduction  
233 with hydrogen gas in the presence of an iron catalyst at  $600^\circ C$ . Results were reported in percent  
234 Modern carbon (pMC) normalized against the  $\delta^{13}C$  of the graphite, with an average  $1\sigma$  error of

235 the AMS readings at  $\pm 0.3$  pMC. Radiocarbon age calculations are presented as ‘conventional  
236 radiocarbon ages’ (years Before Present)<sup>45</sup> and not calendar ages using the equation:

237 
$$^{14}\text{C age} = -8033 \times \ln\left[\frac{(1 + \Delta^{14}\text{C}_{\text{initial}} / 1000)}{(1 + \Delta^{14}\text{C}_{\text{atm}} / 1000)}\right] \text{ } ^{14}\text{C years}$$

238 with  $\Delta^{14}\text{C}_{\text{initial}}$  as the initial radiocarbon content and  $\Delta^{14}\text{C}_{\text{atm}}$  as the radiocarbon content of the  
239 atmosphere at the time of deposition.

## 240 **Results and Discussion**

### 241 Treatment application and labeled exports

242 The pulse of labeled MPB-C produced by the *in situ* MPB community ( $1549 \mu\text{mol } ^{13}\text{C m}^{-2}$   
243 added as OC) quickly underwent processing by the microbial community. Significantly more of  
244 this newly fixed C was remineralized and exported as  $\text{DI}^{13}\text{C}$  under increased nutrient availability  
245 than under ambient conditions (two-way ANOVA: treatment  $F_{1,19}=12.3, p<0.01$ , day  $F_{4,19}=2.4$ ,  
246  $p=0.1$ , interaction  $p=0.08$ ; Fig. 3A). Increased export in the elevated treatment was observed at  
247 0.5 d after nutrient addition and maintained for at least 10.5 d. Cumulative export of  $\text{DO}^{13}\text{C}$  was  
248 similar across treatments, with lower  $\text{DO}^{13}\text{C}$  fluxes than  $\text{DI}^{13}\text{C}$  fluxes, and increased significantly  
249 over 10.5 d (two-way ANOVA: treatment  $F_{1,19}=4.3, p=0.02$ , day  $F_{4,19}=9.4, p<0.01$ , interaction  
250  $p=0.9$ ; Fig.3B).

### 251 Increased DOC Efflux

252 MPB-C stimulated breakdown and export of pre-existing sediment OM and increased the  
253 efflux of DOC derived from this material to the water column under increased nutrient  
254 concentrations (Elevated treatment, 10.5 d, Fig. 4B). Increased efflux of DOC from pre-existing  
255 sediment OM in the elevated treatment was significantly in excess of the ambient treatment

256 across 10.5 d (two-way ANOVA: treatment  $F_{1,19}=51.2$ ;  $p<0.001$ , day  $F_{4,19}=27.6$ ,  $p<0.001$ ;  
257 interaction  $p<0.001$ ). Efflux of DOC derived from sediment OM was larger for the elevated  
258 treatment (1.2-6.6  $\times$ ; Fig. 4B) than for the only positive efflux observed within the ambient  
259 treatment (10.5 d;  $670 \pm 212 \mu\text{mol C m}^{-2} \text{ h}^{-1}$ ; Fig. 4B). Because we were able to partition  
260 completely both the non-labeled and labeled pools of C that composed DIC and DOC effluxes,  
261 we were able to identify a substantial increase in the efflux of unlabeled DOC, which comprised  
262 86% of the cumulative total C export (Elevated 10.5 d, Fig. 4B) under increased nutrient  
263 availability. The statistically significant differences in fluxes between treatments indicate that the  
264 effects observed were robust to low power caused by limited replication ( $n=2$  per time period).

265         Global DOC fluxes from intertidal zones are estimated at 7 to 10 Tg C yr<sup>-1</sup> (minimum to  
266 maximum)<sup>23</sup> with similarly scaled estimates from the elevated treatment in this study resulting in  
267 estimated DOC fluxes of 46.9 to 67.0 Tg C yr<sup>-1</sup>. Although this estimate reflects a 6.7  $\times$  increase  
268 in DOC flux measured for this site-specific study and has considerable associated error, the  
269 magnitude of increased export of DOC from the elevated treatment is concerning given that the  
270 global estimate for total OC burial within coastal sediments is at a similar scale (300 Tg C yr<sup>-1</sup>)<sup>3</sup>.  
271 Our estimate of enhanced DOC flux likely overemphasizes the global role of PEs, given that not  
272 all intertidal zones are microphytobenthos-dominated. However, our estimate would  
273 conservatively decrease current organic carbon burial estimates by ~8 to 11% at a spatial  
274 occurrence of 50%. The scale of this effect highlights that the DOC flux increase stimulated by  
275 PEs are potentially globally significant for enhancing the removal of refractory carbon from  
276 coastal sediments.

277

278 Characterization of exported DOC

279 To verify that effluxed material resulted from the additional breakdown of old and  
280 refractory sediment OM, we used three approaches: UV-visible absorption spectra, C/N, and  
281  $\Delta^{14}\text{C}$  dating. We characterized the DOC efflux for both treatments by UV-visible absorption  
282 spectra, using both slope ratio ( $S_R$ )<sup>24</sup> and SUVA 254<sup>25</sup> to characterize size and relative  
283 aromaticity of the molecules comprising the effluxed DOC. Molecules comprising the DOC  
284 efflux within the elevated treatment had higher C/N ratios, a reduced molecular size, and  
285 increased aromaticity (Fig. 5). These combined results indicate that the DOC produced over 10.5  
286 d was more refractory than control DOC effluxes. Although increased DOC effluxes can be  
287 associated with hypoxic or anoxic events in the sediment<sup>26</sup>, the increased export of more  
288 refractory molecules in the elevated treatment here occurred under oxic conditions (lowest  $\text{O}_2$   
289 measurement  $4.85 \text{ mg L}^{-1}$  at the end of dark period at 10.5 d) and DOC fluxes were comparable  
290 during dark and light periods. It is therefore unlikely that increased DOC efflux was due to either  
291 the development of hypoxic or anoxic conditions, or large shifts in redox conditions in the 20 cm  
292 sediment cores.

293 The old radiocarbon age ( $6855 \pm 120$  years BP) for DOC in the elevated treatment further  
294 showed that old sediment OM was broken down and exported as DOC as a result of PE. The old  
295 age of DOC resulting from the breakdown of sediment OM at the study site suggests that the  
296 material forming the sediment was composed of older scour material deposited on the mudflat.  
297 Flooding within the Richmond River occurs at regular intervals<sup>27,28</sup> and dating of basal core  
298 organic matter just upstream from our study site showed an age of 5,312 - 5,583 y BP<sup>29</sup>, which is  
299 similar to the age of the effluxed DOC. Given the tendency for material composed of older  $\Delta^{14}\text{C}$   
300 to be less photo-reactive and bioavailable, and the refractory nature of the characterized

301 compounds, the exported material is likely directly transported to the coastal shelf with minimal  
302 reworking after hydrolysis by heterotrophic bacteria in the sediment.

303 Is this priming?

304         The high C:N ratio, small molecular size, and radiocarbon age of effluxed DOC provide  
305 compelling evidence that PE occurred within the intertidal sediments in this study. Microbial  
306 processing of MPB-C under elevated nutrient loads resulted in carbon released from breakdown  
307 of older sediment OM via hydrolysis<sup>30</sup> that was largely exported via DOC effluxes (Fig. 1B). The  
308 combination of a labile pulse of C, enhanced by increased nutrient availability, stimulated  
309 microbial degradation of older refractory OM, likely through increased bacterial production of  
310 hydrolytic extracellular enzymes<sup>31</sup>. Although we did not measure enzyme activity, increased  
311 breakdown of sediment OM was indicated by the old radiocarbon age and increased aromaticity  
312 of the increased DOC effluxes produced in the elevated treatment (Fig. 5A & B). The pulse of  
313 labile MPB-C was strongly retained within sediment OM in both treatments across 3.5 d (Fig. 3),  
314 with relatively low effluxes for  $DI^{13}C$  and  $DO^{13}C$  across this time resulting in relatively long  
315 estimates for MPB-C turnover (419 d ambient vs 199 d elevated)<sup>32</sup>. Strong short-term retention  
316 of MPB-C in both treatments indicates that the microbial community readily utilized the newly  
317 produced labile  $^{13}C$  and subsequently recycled respired  $DI^{13}C$  to support productivity.

318         Respiration of older sediment OM provided increased DIC to support MPB productivity  
319 (Fig. 3A) within a system that has been previously found to be DIC-limited<sup>33</sup>. Algal production  
320 supported by recycled DIC was captured by oxygen fluxes and production to respiration  
321 measurements, as increased bacterial respiration of OM increasingly offset initial productivity in  
322 the elevated treatment (Supplemental Fig. 1). However, these dynamics are not supported by



323 consideration of DIC fluxes alone, as the considerable primary productivity that occurred during  
324 light periods offset the respired carbon that would have been exported in a less productive  
325 system. A potential solution to this problem could be to include DOC exports from sediment  
326 OM, a byproduct of remineralization that has not previously been considered in evaluation of  
327 PEs (Fig. 3B & 4B). It is important to acknowledge that DOC exports can also consist of MPB  
328 exudates, therefore exported DOC must be characterized as having arisen from bacterial  
329 remineralization of sediment OM. Characterization of DOC effluxes (using both molecular and  
330 radiocarbon techniques) serves to confirm that the DOC is not predominately composed of labile  
331 compounds copiously produced by MPB. Inclusion of the fluxes of DIC and DOC together  
332 enabled more complete accounting of the export of C that arose during a priming event within a  
333 highly productive benthic environment.

334 We posit that some of the difficulty identifying positive PEs in aquatic systems<sup>11</sup> may be  
335 due to the examination of solely heterotrophic relationships during the processing of OM.  
336 Exclusion of any interactions with primary producers misses potential co-metabolism or  
337 processes that occur in situ (Fig. 1 bottom), including the recapture and recycling of the products  
338 of PE (CO<sub>2</sub>/DIC) during high productivity. This is largely an artefact of PE studies having been  
339 developed in soils<sup>5,34</sup> where remineralization is the sole process affecting the respiratory CO<sub>2</sub>  
340 evolution, primary producers (MPB) are absent, and CO<sub>2</sub> is easily monitored as a production  
341 only function (Fig. 1 top). In aquatic systems, the evolution of CO<sub>2</sub> is likely to be at least  
342 partially offset by primary productivity in many settings where priming is likely to occur (e.g.  
343 shallow benthic microbial communities, suspended estuarine microbial communities). Therefore  
344 CO<sub>2</sub> production alone does not adequately represent microbial heterotrophic processing in  
345 euphotic systems. Further development of a standard metric for quantifying potential PEs that

346 accounts for both respiration and production would be useful in investigating the dynamics of co-  
347 metabolism in communities containing both microbial producers and bacterial heterotrophs.

#### 348 Implications

349 This study suggests that nutrient enrichment of coastal systems<sup>35</sup> may be an additive  
350 factor in stimulating the decomposition and export of C from sediment OM. Increased nutrient  
351 availability stimulated increased efflux of DOC sourced from older OM most likely through  
352 increased bioavailability of OM to heterotrophic bacteria. Bacterial processing increased export  
353 of sediment OC that was previously immobilized and unavailable for processing and export. DIC  
354 and nutrients that arose from bacterial remineralization likely supported MPB productivity and  
355 were recycled within the sediment by co-metabolism within the microbial community. Increased  
356 microbial recycling resulted in increased contribution of uncharacterized material to <sup>13</sup>C within  
357 sediment OM in the elevated treatment<sup>32</sup>. Therefore, inclusion of the byproducts of  
358 remineralization from sediment OM (DOC) allows for more complete accounting of the C arising  
359 from PEs, especially in highly productive systems.

360 Increased remineralization and export of DOC under elevated nutrient conditions  
361 provides a potential PE resulting in increased C export from estuarine sediments to the  
362 continental shelves and should be further considered within blue carbon inventories for coastal  
363 sediments. This study has shown that immobilized OM in shallow photic sediments that is  
364 otherwise considered to be non-reactive and buried may become bioavailable through the  
365 combination of benthic algal production and elevated nutrient inputs. Inclusion of the DOC  
366 export from sediment OM in priming studies may allow identification of PEs in systems that

367 include primary producers. Further development of this method has considerable potential for  
368 broad application to aquatic systems containing algal producers.

## 369 **References**

- 370 1 Glud, R. N. Oxygen dynamics of marine sediments. *Marine Biology Research* **4**, 243-289 (2008).  
371 2 Raymond, P. A. & Bauer, J. E. Use of  $^{14}\text{C}$  and  $^{13}\text{C}$  natural abundances for evaluating riverine,  
372 estuarine, and coastal DOC and POC sources and cycling: a review and synthesis. *Organic*  
373 *Geochemistry* **32**, 469-485 (2001).  
374 3 Bauer, J. E. *et al.* The changing carbon cycle of the coastal ocean. *Nature* **504**, 61-70 (2013).  
375 4 Cai, W.-J. Estuarine and coastal ocean carbon paradox:  $\text{CO}_2$  sinks or sites of terrestrial carbon  
376 incineration? *Annual Review of Marine Science* **3**, 123-145 (2011).  
377 5 Kuzyakov, Y., Friedel, J. & Stahr, K. Review of mechanisms and quantification of priming effects.  
378 *Soil Biology and Biochemistry* **32**, 1485-1498 (2000).  
379 6 Blagodatskaya, E. & Kuzyakov, Y. Mechanisms of real and apparent priming effects and their  
380 dependence on soil microbial biomass and community structure: critical review. *Biology and*  
381 *Fertility of Soils* **45** (2008).  
382 7 Bianchi, T. S. The role of terrestrially derived organic carbon in the coastal ocean: a changing  
383 paradigm and the priming effect. *Proceedings of the National Academy of Sciences* **108**, 19473-  
384 19481 (2011).  
385 8 Hee, C. A., Pease, T. K., Alperin, M. J. & Martens, C. S. Dissolved organic carbon production and  
386 consumption in anoxic marine sediments: A pulsed-tracer experiment. *Limnology and*  
387 *oceanography* **46**, 1908-1920 (2001).  
388 9 van Nugteren, P. *et al.* Seafloor ecosystem functioning: the importance of organic matter  
389 priming. *Marine Biology* **156**, 2277-2287 (2009).  
390 10 Bianchi, T. S. *et al.* Positive priming of terrestrially derived dissolved organic matter in a  
391 freshwater microcosm system. *Geophysical Research Letters* **42**, 5460-5467 (2015).  
392 11 Bengtsson, M. M., Attermeyer, K. & Catalán, N. Interactive effects on organic matter processing  
393 from soils to the ocean: are priming effects relevant in aquatic ecosystems? *Hydrobiologia*  
394 (2018).  
395 12 Hannides, A. K. & Aller, R. C. Priming effect of benthic gastropod mucus on sedimentary organic  
396 matter remineralization. *Limnology and Oceanography* **61**, 1640-1650 (2016).  
397 13 Gontikaki, E., Thornton, B., Cornulier, T. & Witte, U. Occurrence of priming in the degradation of  
398 lignocellulose in marine sediments. *PLoS ONE* **10** (2015).  
399 14 Koch, B. P., Kattner, G., Witt, M. & Passow, U. Molecular insights into the microbial formation of  
400 marine dissolved organic matter: recalcitrant or labile? *Biogeosciences* **11**, 4173-4190 (2014).  
401 15 Catalán, N., Kellerman, A. M., Peter, H., Carmona, F. & Tranvik, L. J. Absence of a priming effect  
402 on dissolved organic carbon degradation in lake water. *Limnology and Oceanography* **60**, 159-  
403 168 (2015).  
404 16 Bengtsson, M. M. *et al.* No evidence of aquatic priming effects in hyporheic zone microcosms.  
405 *Scientific Reports* **4**, 5187 (2014).  
406 17 Danger, M. *et al.* Benthic algae stimulate leaf litter decomposition in detritus-based headwater  
407 streams: a case of aquatic priming. *Ecology* **94**, 1604-1613 (2013).  
408 18 Guenet, B. *et al.* Fast mineralization of land-born C in inland waters: First experimental  
409 evidences of aquatic priming effect. *Hydrobiologia* **721**, 35-44 (2014).

- 410 19 Oakes, J. M., Eyre, B., D., Middelburg, J. J. & Boschker, H. T. S. Composition, production, and loss  
411 of carbohydrates in subtropical shallow subtidal sandy sediments: rapid processing and long-  
412 term retention revealed by <sup>13</sup>C-labeling. *Limnology and Oceanography* **55**, 2126-2138 (2010).
- 413 20 Kristensen, E. & Holmer, M. Decomposition of plant materials in marine sediment exposed to  
414 different electron acceptors (O<sub>2</sub>, NO<sub>3</sub><sup>-</sup>, and SO<sub>4</sub><sup>2-</sup>), with emphasis on substrate origin,  
415 degradation kinetics, and the role of bioturbation. *Geochimica et Cosmochimica Acta* **65**, 419-  
416 433 (2001).
- 417 21 ANZECC. *Australia and New Zealand guidelines for fresh and marine water quality*,  
418 <<https://www.waterquality.gov.au/guidelines/anz-fresh-marine>> (2018).
- 419 22 Macreadie, P. I. *et al.* The future of Blue Carbon science. *Nature communications* **10**, 1-13  
420 (2019).
- 421 23 Maher, D. T. & Eyre, B. D. Benthic fluxes of dissolved organic carbon in three temperate  
422 Australian estuaries: Implications for global estimates of benthic DOC fluxes. *Journal of*  
423 *Geophysical Research: Biogeosciences* **115** (2010).
- 424 24 Helms, J. R. *et al.* Absorption spectral slopes and slope ratios as indicators of molecular weight,  
425 source, and photobleaching of chromophoric dissolved organic matter. *Limnology and*  
426 *Oceanography* **53**, 955-969 (2008).
- 427 25 Weishaar, J. L. *et al.* Evaluation of specific ultraviolet absorbance as an indicator of the chemical  
428 composition and reactivity of dissolved organic carbon. *Environmental Science and Technology*  
429 **37**, 4702-4708 (2003).
- 430 26 Skoog, A. C. & Arias-Esquivel, V. A. The effect of induced anoxia and reoxygenation on benthic  
431 fluxes of organic carbon, phosphate, iron, and manganese. *Science of the total environment* **407**,  
432 6085-6092 (2009).
- 433 27 Eyre, B. Water quality changes in an episodically flushed sub-tropical Australian estuary: A 50  
434 year perspective. *Marine Chemistry* **59**, 177-187 (1997).
- 435 28 McKee, L. J., Eyre, B. D. & Hossain, S. Transport and retention of nitrogen and phosphorus in the  
436 sub-tropical Richmond River estuary, Australia – A budget approach. *Biogeochemistry* **50**, 241-  
437 278 (2000).
- 438 29 Logan, B., Taffs, K., Eyre, B. & Zawadski, A. Assessing changes in nutrient status in the Richmond  
439 River estuary, Australia, using paleolimnological methods. *J Paleolimnol* **46**, 597-611 (2011).
- 440 30 Arnosti, C. Microbial Extracellular Enzymes and the Marine Carbon Cycle. *Annual Review of*  
441 *Marine Science* **3**, 401-425 (2011).
- 442 31 Steen, A. D., Quigley, L. N. M. & Buchan, A. Evidence for the Priming Effect in a Planktonic  
443 Estuarine Microbial Community. *Frontiers in Marine Science* **3** (2016).
- 444 32 Riekenberg, P. M., Oakes, J. M. & Eyre, B. D. Short-term fate of intertidal microphytobenthos  
445 carbon under enhanced nutrient availability: a <sup>13</sup>C pulse-chase experiment. *Biogeosciences* **15**,  
446 2873-2889 (2018).
- 447 33 Oakes, J. M. & Eyre, B. D. Transformation and fate of microphytobenthos carbon in subtropical,  
448 intertidal sediments: Potential for long-term carbon retention revealed by <sup>13</sup>C-labeling.  
449 *Biogeosciences* **11**, 1927-1940 (2014).
- 450 34 Kuz'yakov, Y. Priming effects: Interactions between living and dead organic matter. *Soil Biology*  
451 *and Biochemistry* **42**, 1363-1371 (2010).
- 452 35 Cloern, J. E. Our evolving conceptual model of the coastal eutrophication problem. *Marine*  
453 *ecology progress series* **210**, 223-253 (2001).
- 454 36 Riekenberg, P. M., Oakes, J. M. & Eyre, B. D. Uptake of dissolved organic and inorganic nitrogen  
455 in microalgae-dominated sediment: comparing dark and light *in situ* and *ex situ* additions of <sup>15</sup>N.  
456 *Marine Ecology Progress Series* **571**, 29-42 (2017).

- 457 37 Eyre, B. D. Regional evaluation of nutrient transformation and phytoplankton growth in nine  
458 river-dominated sub-tropical east Australian estuaries. *Marine Ecology Progress Series* **205**, 61-  
459 83 (2000).
- 460 38 Cloern, J. E. *et al.* Human activities and climate variability drive fast-paced change across the  
461 world's estuarine-coastal ecosystems. *Global Change Biology* **22**, 513-529 (2016).
- 462 39 Ferguson, A. J. P., Eyre, B. D. & Gay, J. M. Benthic nutrient fluxes in euphotic sediments along  
463 shallow sub-tropical estuaries, northern New South Wales, Australia. *Aquatic Microbial Ecology*  
464 **37**, 219-235 (2004).
- 465 40 Eyre, B. D., Maher, D. T. & Squire, P. Quantity and quality of organic matter (detritus) drives N<sub>2</sub>  
466 effluxes (net denitrification) across seasons, benthic habitats, and estuaries. *Global*  
467 *Biogeochemical Cycles* **27**, 1083-1095 (2013).
- 468 41 Elvridge, C. D., Keith, D. M., Tuttle, B. T. & Baugh, K. E. Spectral identification of lighting type and  
469 character. *Sensors* **10**, 3961-3988 (2010).
- 470 42 Oakes, J. M., Eyre, B. D., Ross, D. J. & Turner, S. D. Stable Isotopes Trace Estuarine  
471 Transformations of Carbon and Nitrogen from Primary- and Secondary-Treated Paper and Pulp  
472 Mill Effluent. *Environmental Science & Technology* **44**, 7411-7417 (2010).
- 473 43 Jickells, T. & Rae, J. Biogeochemistry of Intertidal Sediments. *Biogeochemistry of Intertidal*  
474 *Sediments*, Edited by TD Jickells and JE Rae, pp. 205. ISBN 0521483069. Cambridge, UK:  
475 Cambridge University Press, June 1997., 205 (1997).
- 476 44 Fink, D. *et al.* The ANTARES AMS facility at ANSTO. *Nuclear Instruments and Methods in Physics*  
477 *Research Section B: Beam Interactions with Materials and Atoms* **223–224**, 109-115 (2004).
- 478 45 Stuiver, M. & Polach, H. A. Reporting of <sup>14</sup>C data. *Radiocarbon* **19**, 355-363 (1977).

479

480 Acknowledgements: We thank I. Alexander, M. Carvalho, N. Carlson-Perret, R. Murray, B.  
481 Riekenberg, and J. Riekenberg for technical assistance and field support. Funding: This work  
482 was supported by grants from the Australian Research Council (ARC), specifically an Early  
483 Career Research Award to J.M.O (DE120101290) and a Discovery Project to B.D.E.  
484 (DP160100248). Author contributions: P.M.R., J.M.O., and B.D.E. conceived the project and  
485 designed the experiment, P.M.R. and J.M.O. performed the experiment processed samples,  
486 P.M.R., J.M.O. and B.D.E. analyzed the data, and P.M.R. wrote the manuscript with input from  
487 J.M.O. and B.D.E. Competing Interests: The authors declare that they have no competing  
488 interests. Data and materials availability: All data needed for evaluation of the conclusions within  
489 this paper are present in the paper and/or Supplementary Materials, but additional data is  
490 available from authors upon request.

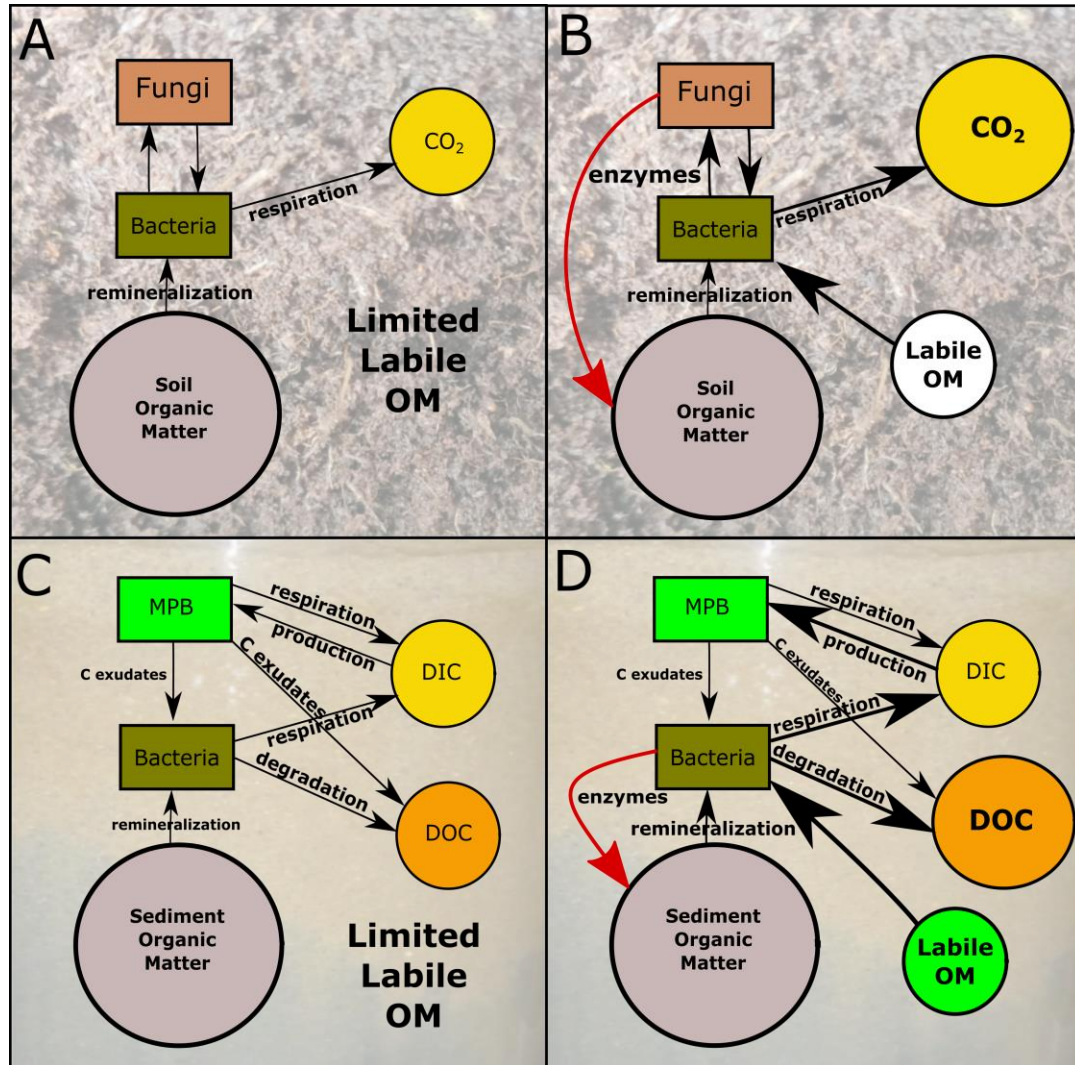
491

492 Supplementary Materials:

493 Table S1:  $\delta^{13}\text{C}$  (‰) values for DIC and DOC diel fluxes across the 10.5 d incubation period.

494 S1: Oxygen fluxes and production/respiration measurements.

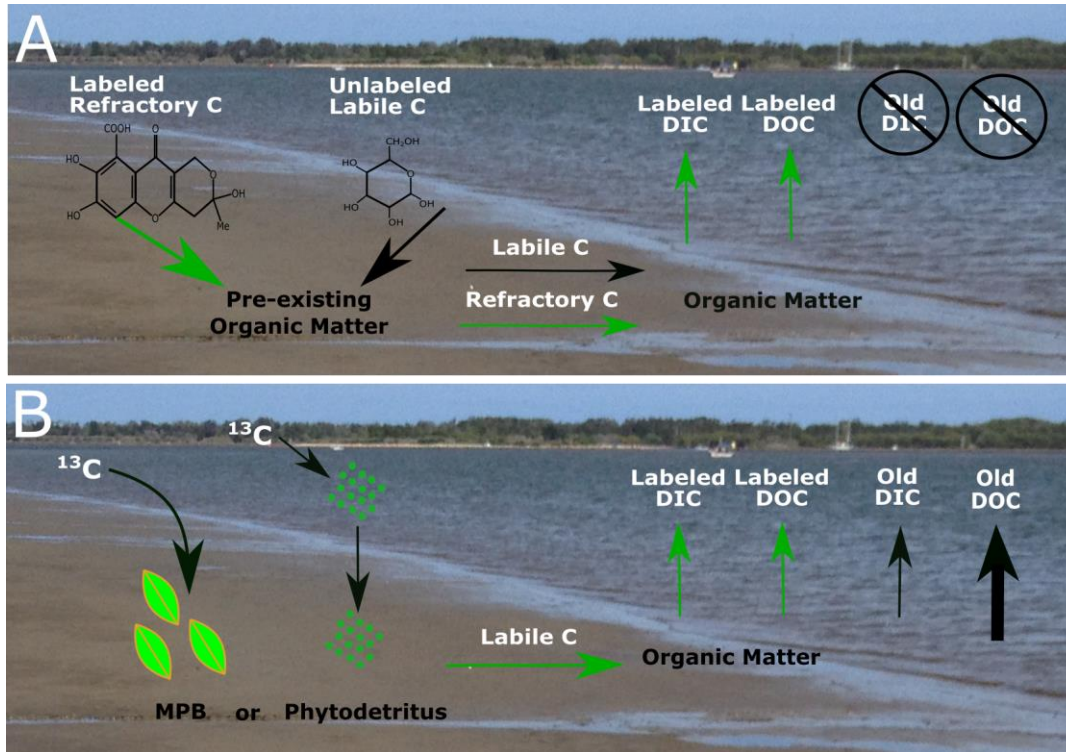
495 **Figures**



496

497 **Figure 1:** Fluxes of C within heterotrophic dominated soil (top) and autotrophic dominated  
498 benthic sediment (bottom) under normal (left panels A and C) and B) and priming (right panels,  
499 B and D) scenarios. The red arrows indicate stimulated production of hydrolytic enzymes by  
500 fungi (B) and heterotrophic bacteria (D). Note the bi-directional flows of carbon associated with  
501 productive benthic sediments. Soil conceptual diagram (top) adapted from Kuzyakov (2010)  
502 (30). Photo credit: Philip Riekenberg, NIOZ.

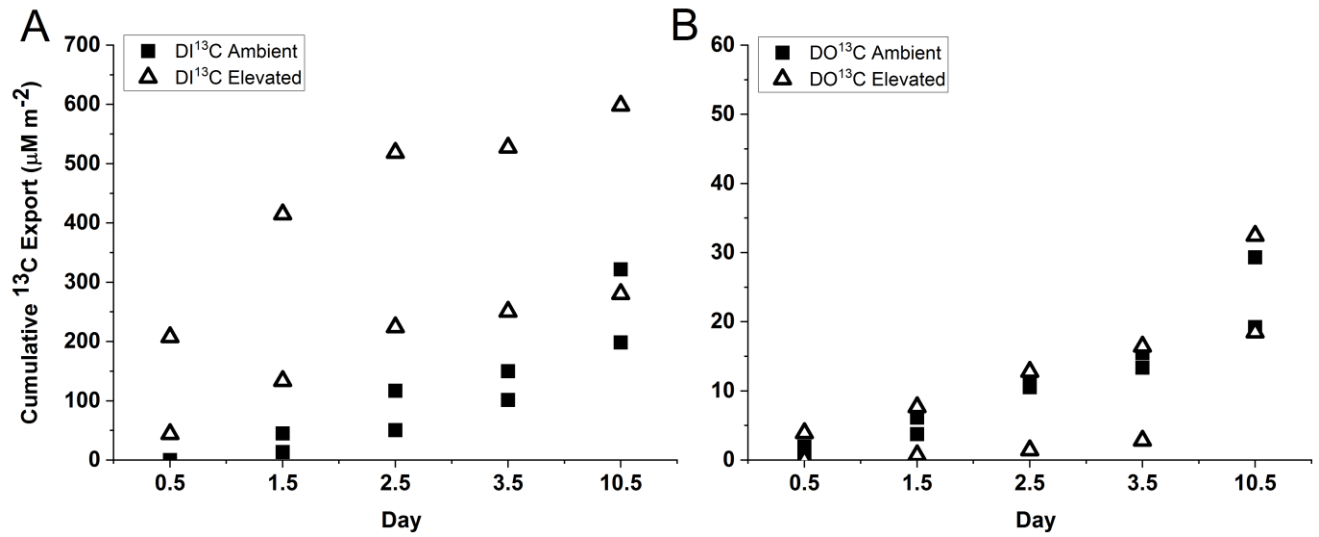
503



504

505 **Figure 2:** Method diagram comparing priming addition methods. A) Priming experiments  
506 typically introduce <sup>13</sup>C-labeled labile and/or refractory material to sediment OM. The export of  
507 labeled material can then be traced as additional export occurs, but the unlabeled OM pool is  
508 muddled, making it impossible to track decomposition of pre-existing sediment OM. B)  
509 Additions of <sup>13</sup>C-labeled algal-derived carbon from prepared phytodetritus or label additions  
510 processed by the *in situ* microphytobenthos community allow for simultaneous quantification of  
511 both non-labeled and labeled DIC and DOC effluxes. In the current study the combined addition  
512 of microphytobenthos (MPB) derived C and nutrients enhanced export of both pre-existing C  
513 from sediment OM, primarily as DOC, as well as labeled DIC. Photo credit: Philip Riekenberg,  
514 NIOZ.

515



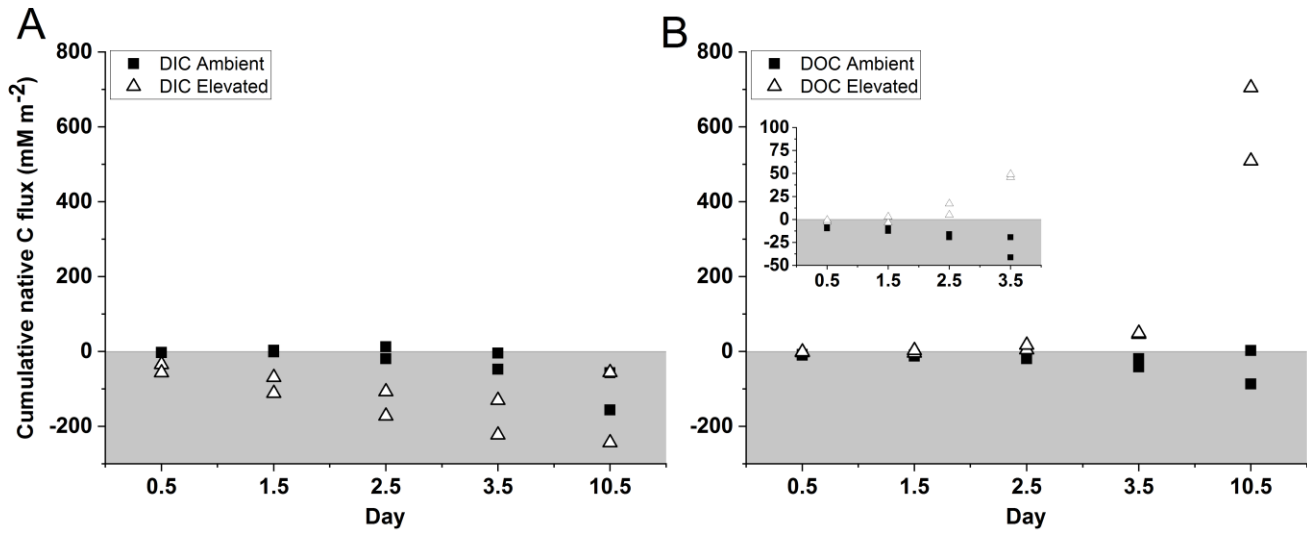
5

517 **Figure 3:** Cumulative export of A) DI<sup>13</sup>C and B) DO<sup>13</sup>C from the sediment for individual  
518 replicates within each treatment. Export of <sup>13</sup>C represents microbial utilization and export of  
519 fixed microphytobenthos carbon from the treatment application. DI<sup>13</sup>C export was significantly  
520 higher in the elevated treatment than ambient (two-way ANOVA: treatment  $F_{1,19}=12.3$ ,  $p<0.01$ ,  
521 day  $F_{4,19}=2.4$ ,  $p=0.1$ , interaction  $p=0.08$ ).

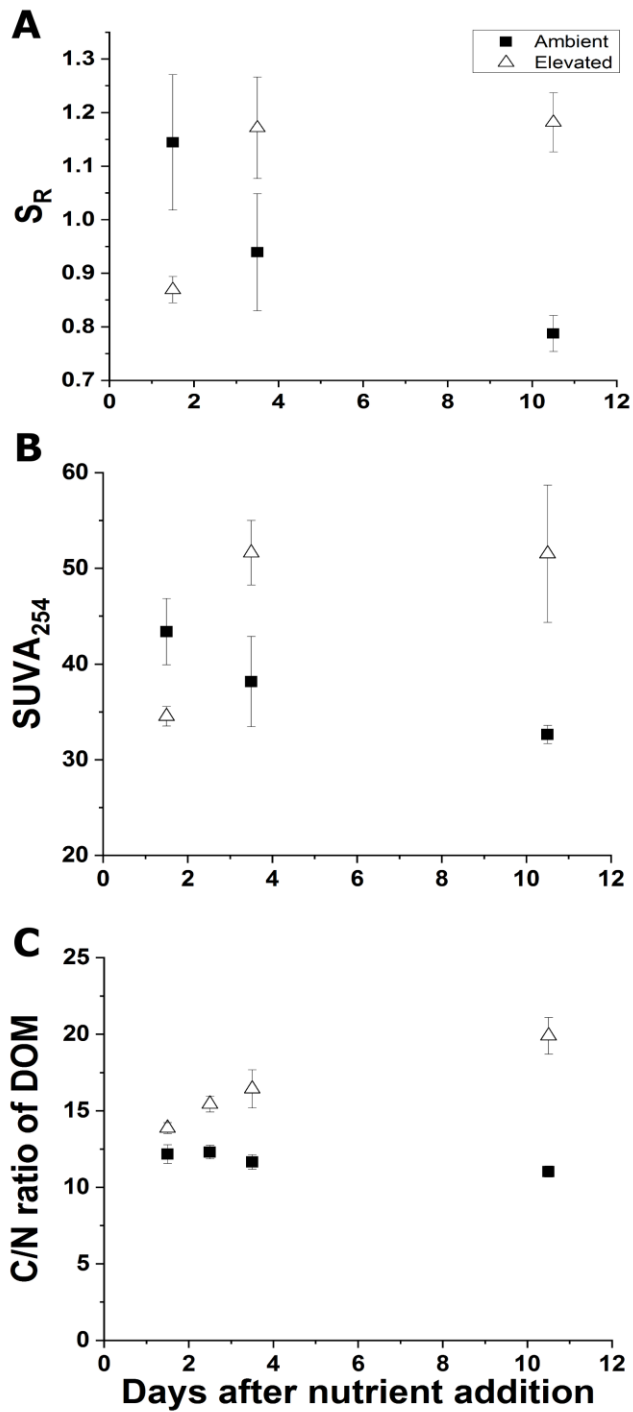
522

523





525 **Figure 4:** Cumulative flux of non-labeled A) DIC and B) DOC. DOC flux was significantly  
526 higher in the elevated treatment than ambient (two-way ANOVA: treatment  $F_{1,19}=51.2$ ;  $p<0.001$ ,  
527 day  $F_{4,19}=27.6$ ,  $p<0.001$ ; interaction  $p<0.001$ ) and represents export derived from pre-existing  
528 sediment OM. Inset graph highlights the differences between ambient and elevated fluxes of  
529 DOC at 0.5-3.5 d. Grey region indicates uptake of carbon.



530

531 **Figure 5:** Characterization of DOC efflux via A) slope ratio of DOC for both treatments, B)  
532  $SUVA_{254}$  of DOC for both treatments, and C) C/N ratios for dissolved organic material efflux.

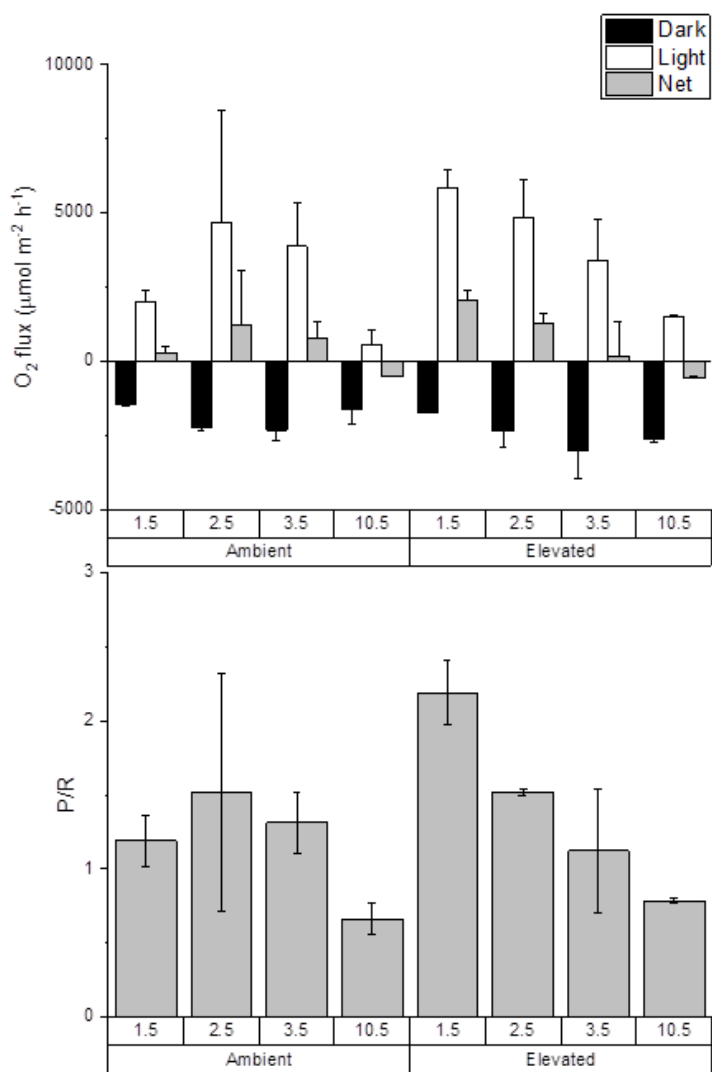
533 All measurements for indicated treatments were performed on duplicate cores (mean $\pm$ SD).

534 **Supplemental Material**

Treatment	Day	Replicate	DOC			DIC		
			Initial	Dark	Light	Initial	Dark	Light
Ambient	1.5	1	-18.0	-13.2	-11.4	21.6	24.5	14.3
Ambient	1.5	2	-19.2	-15.0	-13.7	14.0	24.5	21.8
Ambient	2.5	1	-16.7	-11.2	-9.7	11.8	15.9	16.4
Ambient	2.5	2	-17.0	-12.6	-9.9	12.8	17.4	18.3
Ambient	3.5	1	-11.9	-6.2	-9.0	14.6	20.2	14.7
Ambient	3.5	2	-13.6	-9.2	-11.0	13.0	14.0	12.8
Ambient	10.5	1	-18.0	-15.2	-15.9	11.3	9.8	10.4
Ambient	10.5	2	-16.7	-14.1	-14.0	11.0	11.1	10.8
Elevated	1.5	1	-19.6	-15.3	-18.1	15.2	8.0	19.7
Elevated	1.5	2	-19.5	-15.6	-14.3	8.3	18.9	22.4
Elevated	2.5	1	-19.7	-20.4	-20.6	7.2	5.9	5.2
Elevated	2.5	2	-17.4	-10.9	-10.4	10.4	16.5	15.5
Elevated	3.5	1	-16.3	-11.8	-14.4	9.6	11.0	11.3
Elevated	3.5	2	-18.4	-19.0	-20.3	9.1	8.7	9.3
Elevated	10.5	1	-14.9	-21.6	-20.1	9.2	8.7	8.9
Elevated	10.5	2	-13.3	-17.2	-20.2	9.5	9.3	7.8

535

536 **Supplemental Table 1:  $\delta^{13}\text{C}$  (‰) values for DIC and DOC diel fluxes across the 10.5 d**  
 537 **incubation period. Initial measurements represent the initial dark period measurement at**  
 538 **dusk, “Dark” measurements are the end of the dark period measured at dawn, and “Light”**  
 539 **measurements represent the end of the photoperiod prior to supersaturation of oxygen**  
 540 **(>100% dissolved oxygen) as required for a simultaneous measurement.**



541

542 **Supplemental Figure 1: Oxygen fluxes and production/respiration measurements.** All

543 measurements for indicated treatments were performed on duplicate cores.

544

545

546